Original research or treatment paper

Use of imaging spectroscopy, fiber optic reflectance spectroscopy, and X-ray fluorescence to map and identify pigments in illuminated manuscripts

John K. Delaney[1], Paola Ricciardi[1], Lisha Deming Glinsman[1], Michelle Facini[2], Mathieu Thoury[1], Michael Palmer[1], E. René de la Rie[1]

[1]Scientific Research Department, National Gallery of Art, Washington, DC, USA, [2]Paper Conservation Department, National Gallery of Art, Washington, DC, USA

A paradigm using multispectral visible and near-infrared imaging spectroscopy is presented to semi-automatically create unbiased spectral maps that guide the site selection for *in situ* analytical methods (e.g. fiber optic reflectance spectroscopy and X-ray fluorescence) in order to identify and map pigments in illuminated manuscripts. This approach uses low spectral resolution imaging spectroscopy to create maps of areas having the same spectral characteristics. This paradigm is demonstrated by analysis of the illuminated manuscript leaf *Christ in Majesty with Twelve Apostles* (workshop of Pacino di Buonaguida, c. 1320). Using this approach the primary pigments are mapped and identified as azurite, lead-tin yellow, red lead, a red lake (likely insect-derived), a copper-containing green, brown iron oxide, and lead white. Moreover, small amounts of natural ultramarine were found to be used to enhance the blue fields around Christ, and a red lake was used to highlight different colors. These results suggest that the proposed paradigm offers an improved approach to the comprehensive study of illuminated manuscripts by comparison with site-specific analytical methods alone. The choice of broad spectral bands proves successful, given the limited palette in illuminated manuscripts, and permits operation at the low light intensity required for examination of manuscripts.

Keywords: X-ray fluorescence, Imaging spectroscopy, Fiber optics reflectance spectroscopy, Illuminated manuscripts

Introduction

Spectral imaging for art conservation is an active field (Delaney *et al.*, 2005; Fischer & Kakoulli, 2006; Klein *et al.*, 2008; Zhao *et al.*, 2008, Delaney *et al.*, 2009a, b, 2010; Padoan *et al.*, 2010) and an important distinction still exists between radiometrically un-calibrated spectral imaging and imaging spectroscopy (Delaney *et al.*, 2005; Klein *et al.*, 2008). The former mainly uses the spectral differences of artist's materials to enhance the visualization of specific features by creating false color composites, difference images, or principal component images, to separate for example iron-based from carbon-based ink writing (Mrusek *et al.*, 1995; Havermans *et al.*, 2003; France, 2011). Such spectral imaging can be more accurately referred to as multi- or hyper-band imaging, especially if X-ray or luminescence images are included. Imaging spectroscopy, on the other hand, seeks to use the spectra from each pixel for a variety of tasks, from improving color accuracy (Burns, 2005) to the more challenging mapping and identification of the primary colorants (Delaney *et al.*, 2010). In this paper, the focus is on reflectance imaging spectroscopy, the capture of spectral images in contiguous spectral bands that have been radiometrically calibrated to apparent reflectance in order to map areas having similar reflectance spectra.

Only a handful of studies to date have successfully demonstrated the benefits of applying imaging spectroscopy to the study of artworks. Key to success is the acquisition of high-quality spectra in the visible and near infrared (NIR), specifically in the 400 to ~1650 nm spectral range (Baronti *et al.*, 1998; Casini *et al.*, 1999, 2005; Delaney *et al.*, 2005, 2009b, 2010). Because high light levels are required to obtain satisfactory spectra, it is not surprising that these studies have been limited to paintings. The few studies on works on paper and parchment have mostly explored

Correspondence to: John K. Delaney, Scientific Research Department, National Gallery of Art, 4th and Constitution Avenue NW, Washington, DC 20565, USA. Email: J-Delaney@NGA.GOV

Received January 2012; revised paper accepted December 2012
DOI 10.1179/2047058412Y.0000000078

the visible range and part of the NIR (750–1000 nm), and typically have low spectral resolution, but high spatial resolution. In most of these cases, the image processing has been limited to analysis of a handful of spectra and some principal component analysis (Melessanaki *et al*., 2001; Attas *et al*., 2003). Given the desire to minimize light exposure during analysis of light-sensitive artworks (Ashley-Smith *et al*., 2002), one is forced into a trade between spatial and spectral resolution (Delaney *et al*., 2005; Dirk *et al*., 2009). That is, for fixed lighting conditions one has to trade the size of pixel at the artwork (spatial sampling) for width of the spectral sampling. Thus, if one desires high-resolution spectra one has to give up on small spatial sampling and vice versa.

In a recent study (Ricciardi *et al*., 2009), we demonstrated that the limited set of pigments used in manuscript illuminations can be at least separated and sometimes identified, even when mixed, by acquiring images at moderate spectral sampling intervals (50 nm) under low light levels (~150 lux) while having high spatial sampling (~250 pixels per in). Similar to prior studies (Casini *et al*., 1999; Bacci *et al*., 2007a, b; Aceto *et al*., 2008; Appolonia *et al*., 2009), the work further showed that by using the *in situ* techniques of fiber optic reflectance spectroscopy (FORS) and X-ray fluorescence (XRF) together, pigments can be identified with a high degree of confidence. This work also showed that the loss in spectral information because of not using hyperspectral imaging did not impact the ability to form detailed maps, and the use of FORS at sites defined by the maps provided the high-resolution spectral information needed. However, in that case the analysis of the image cube was done by human trial and error, i.e. the endmember spectra were manually selected.

In this work, the spectral imaging processing previously used for the objective mapping and identification of pigments in a painting by Pablo Picasso (Delaney *et al*., 2009a, b) was applied to a multispectral reflectance cube acquired on an illuminated manuscript leaf (Delaney *et al*., 2009a). The results of the previous study suggest that an automatic, and unbiased, processing method can be used to make preliminary maps to guide more time consuming but more chemically accurate site-specific methods such as FORS, XRF, and Raman spectroscopy.

The illuminated manuscript leaf studied here is from a *laudario*, or choir book, of the Compagnia di Sant'Agnese illustrated by the workshop of Pacino di Buonaguida, an influential panel painter and one of the most prolific Florentine illuminators in the first half of the fourteenth century (Kanter *et al*., 1994). Scholars believe that during the period of the Napoleonic war, this *laudario* was transported out of Italy, then unbound, and sold in London in the first half of the eighteenth century (Panayotova, 2009). The frontispiece illumination titled *Christ in Majesty with Twelve Apostles* had been cut away along its perimeter border from its original choir leaf before being acquired by Lessing J. Rosenwald (1891–1979) and bequeathed to the National Gallery of Art, Washington, DC in 1952.

The illuminated miniature depicts Christ, wearing a white mantle over a yellow-green robe enthroned in a blue *mandorla* surrounded by the 12 apostles in prayer dressed in pink, orange-red, brown, and green robes (Fig. 1A). The illumination is in very good condition despite some abrasion of the gold leaf and small areas of loss. The color palette is strong and bright and the figures, shown mostly in profile, appear as fresh and elegant as when the artist painted them (Nordenfalk, 1975). The miniature is consistent in both style and format with the other 27 identified works depicting the religious calendar of worship in the *laudario*. One of the most richly decorated manuscripts of the Florentine Trecento, this exceptional choir book was among the last great projects left unfinished by Pacino di Buonaguida at the time of his death. The remainder of the commission was completed by a second artist known as the Master of the Dominican Effigies, Florentine, active c. 1328–1350 (Panayotova, 2009).

Experimental

A homemade, low-cost (<$10k) multispectral camera system, consisting of interference filters and a low-noise Si-CCD, operating from 400 to 950 nm in 12 spectral bands (full-width at half-maximum (FWHM) of 40 nm), is used to obtain both the reflectance and luminescence images (Ricciardi *et al*., 2009, Delaney et al., 2010). For reflectance, the manuscript is illuminated at 160 lux using two 50 W Solux lamps (Solux, Rochester, NY, USA) at ±45° angles from normal. The luminescence image is captured with the same setup described elsewhere (Delaney *et al*., 2010), with spectral radiance of 40 $mW/sr*m^2$. The luminescence image is median filtered (1 pixel) and sharpened, and the optical distortion is removed in Adobe® Photoshop® CS5.

XRF spectra are collected with an ArtTAX Pro XRF Spectrometer (Bruker AXS Inc., Boulder, Co, USA), equipped with a helium flush, a rhodium X-ray tube, and a 60 μm capillary optic lens. The X-ray tube is operated at 50 kV and 200 μA, with a live integration time of 200–600 seconds.

A fiber optic spectroradiometer (FS3, ASD Inc., Boulder, CO, USA) operating from 350 to 2500 nm is used in the same setup described elsewhere (Delaney *et al*., 2010), with a collection area of ~3 mm. The light exposure (~4000 lux) per site is less than 5 seconds.

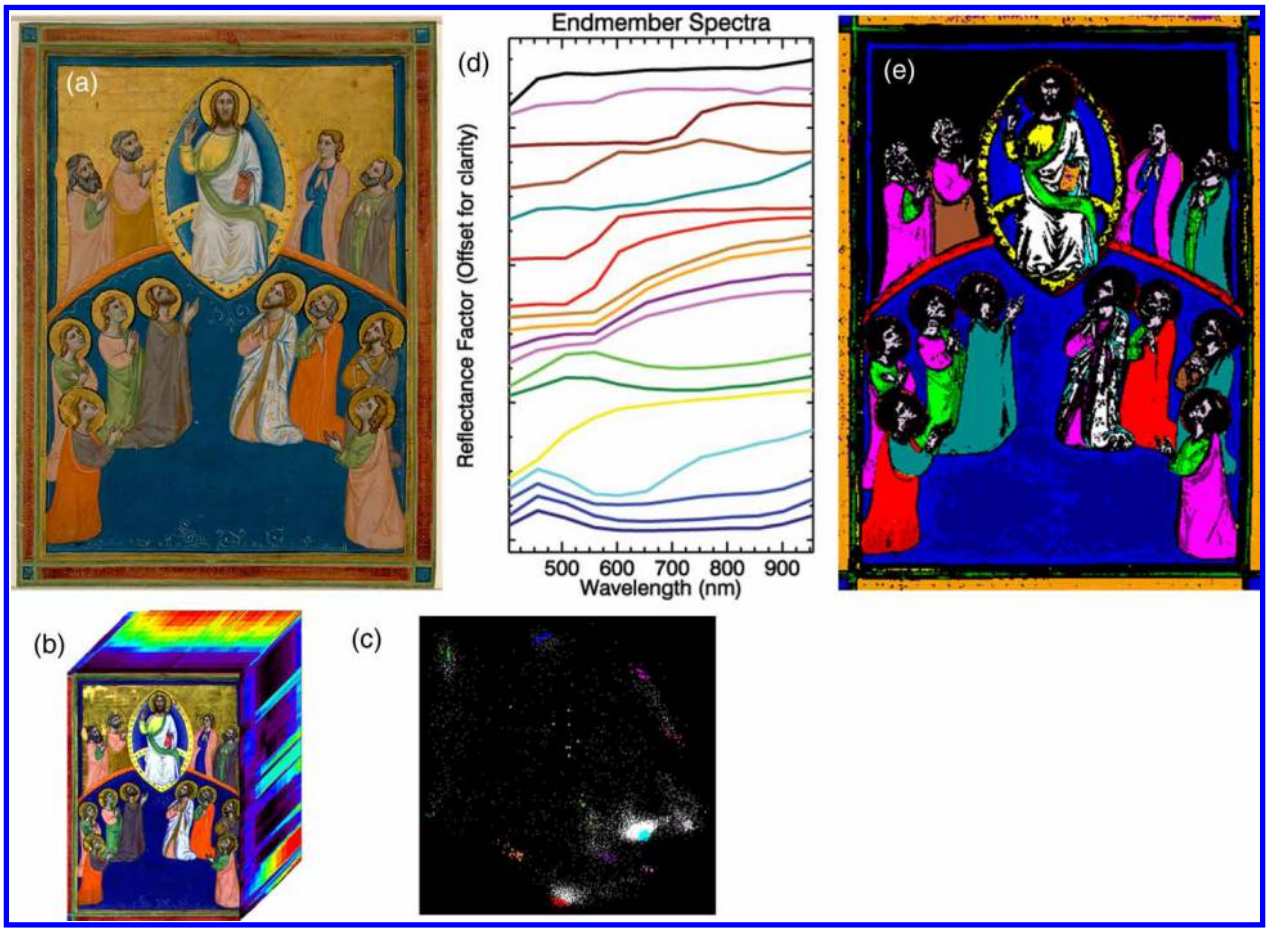

Figure 1 The reflectance imaging spectroscopy workflow. A multispectral reflectance image cube is constructed and analyzed to determine a basis set of reflectance spectra ('endmembers') that best describe the miniature from 400 to 950 nm. The endmembers are used to make spatial maps to guide site selection for FORS and XRF analysis. (A) Workshop of Pacino di Buonaguida, 'Christ in majesty with twelve apostles', c. 1320, Rosenwald collection (photo by Ken Fleisher; image courtesy of the National Gallery of Art, Washington, DC); (B) 3D representation of the image cube; (C) a projection of clusters into two of the 12 dimensions defined by the MNF transform; (D) spectral endmembers obtained by the hyperspectral processing; (E) spatial map of endmembers obtained using the SAM algorithm using angle tolerances in Table 1.

A blue paint sample is analyzed using scanning electron microscopy–energy dispersive X-ray spectroscopy (SEM–EDS; Hitachi S-3400N-INCA, Hitachi High Technologies, Pleasanton, CA, USA) as described elsewhere (Delaney *et al.*, 2010), but excessive charge build up limits the examinations to point analyses.

Results and discussion

The paradigm consists of several steps. First, 12 calibrated reflectance images are acquired using the multispectral camera system at a sampling of 89 pixels per inch at the artwork, or 0.29 mm per pixel. Second, a luminescence image is acquired at 700 nm using the same setup while illuminating with blue-green light. Finally, after creating maps of areas having the same characteristic reflectance spectra, sites are selected for FORS and XRF examination.

Construction of the reflectance image cube

A reflectance image cube consists of a sequential stack of aligned calibrated spectral images running from the blue to the NIR. Each spectral image is flat-fielded using both a dark reference (i.e. lens cap) and a white card (Delaney *et al.*, 2005). This corrects for non-uniform illumination and camera response, as well as integrated detector dark current. The flat-fielded images are then calibrated to reflectance using in-scene diffuse reflectance standards (white and black) (Delaney *et al.*, 2005). The spectral images need to be scaled and aligned to avoid mis-registration, so that accurate reflectance spectra are obtained from the image cube. Several factors give rise to these mis-registrations of the spectral images, but two are most common. The first is residual chromatic aberration (i.e. the variation of lens focal length with wavelength) from the camera lens, which causes each spectral image to have a different scale or relative magnification. This problem is present even if spectral filtering is done at the light source (e.g. use of LEDS, etc.) as opposed to filters at the camera. The second registration error originates from the wedge between the two air/glass surfaces of the

interference filters that can give rise to small image displacements in the order of a few pixels.

The mis-registration can be solved by image processing in several ways. One method consists of manually identifying the pixel positions of similar features in each of the spectral images to generate a set of 'tie points'. Typically tens of tie points are found and used to determine the coefficients of a mathematical function, which enables the images to be brought into alignment. In this study, we have used a Delaunay triangulation-warping algorithm (Delaney *et al.*, 2005). This method fits triangles to selected tie points identified, and interpolates, as needed, points in between them to register the images. This approach was found to yield better results than an often-used general polynomial warping function.

Once the images are flat-fielded, calibrated to reflectance, and registered, the image cube is created (Fig. 1B). To check the quality of the reflectance image cube the reflectance spectra from the white and black diffuse reflectance standards placed in the image scene are examined. The statistical residual standard deviation errors (calculated on the white diffuse reflective standard (97%)) are <0.6% over the spectral range analyzed (400–950 nm), showing the image cube is well calibrated to reflectance.

Analysis of the reflectance image cube

The main goal in analyzing the image cube is the determination of a complete set of spectral endmembers, or the 'basis set' of reflectance spectra that describe the miniature, using an unbiased approach. Given the successful application of hyperspectral algorithms to find endmembers on multispectral data sets, such an approach was taken here, with the same methodology used to separate and map the primary endmembers within Pablo Picasso's 'Harlequin Musician' (Delaney *et al.*, 2010). This algorithm, based on the work of Boardman *et al.* (1995), is called 'hourglass paradigm' and implemented in the ENVI software. To speed data analysis, and further minimize the impact of registration errors, the reflectance image cube is processed with 2×-aggregation, which further reduces the residual reflectance errors per pixel by two-fold.

The paradigm consists of three major steps:

1. The determination of the spectral diversity of the image cube or the number of principal image components, carried out using the minimum noise fraction algorithm, which is a type of principal components analysis. The objective of this algorithm is to determine the level of diversity in the spectral dataset. It yields 'Eigen images' which are orthogonal projections of the pixels in the image cube. The maximum number of Eigen images is the number of spectral bands in the cube. While these images often highlight areas having similar properties they cannot be taken as meaning that these areas were painted with the same materials. In the case presented here, all 12 possible Eigen images showed meaningful information and were retained for the second processing step.
2. The determination of the most spectrally diverse pixels in the image cube. In fact, while the Eigen images demonstrate the diversity of spectral information captured, they do not give insight as to how to group image pixels in terms of similar reflectance spectra. This requires the identification of a subset of spectra in the image cube, which can be used to determine the set of spectral endmembers. This is done using an algorithm called the 'purity pixel index', based on convex geometry, which calculates the pixels having the most unique or most 'pure' spectra in the image cube.
3. The clustering of spectrally diverse pixels in the dimensionality determined by the principal components. Once the 'pure' pixels have been identified, their spectra are plotted in the multidimensional space defined by the Eigen images (in this case 12 dimensions). To assist in the clustering of the endmembers, the ENVI Nd-visualizer is used to manually select the well-separated clusters (Fig. 1C). In the end, 18 clusters were found by this method, giving 18 spectral endmembers that define the image cube (Fig. 1D).

The spectral endmembers can then be compared with spectral databases to identify the pigments present, or used to make 'spectral maps' to guide further studies using other, 'site-specific' methods (such as FORS, XRF, or Raman spectroscopy). The spectral maps are also useful to ensure that the spectral endmembers adequately describe the miniature's surface, i.e. that no endmembers were 'left out' of the analysis. The maps are produced using a spectral angle-mapping (SAM) algorithm. The SAM algorithm identifies pixels in the image cube whose reflectance spectra match those of the endmembers within a specified angle tolerance. The tolerance angles are selected based on an examination of SAM rule images, whose digital count is proportional to the SAM angle. In this study, the resulting spectral maps (Fig. 1E) and angle tolerance values (Table 1) show that the miniature is well described with the exception of areas of exposed parchment and the gold leaf which shows some specular reflectance.

Pigment assignments

Pigments are identified using XRF and FORS data collected at sites defined by the endmember maps (Figs. 1–4, Table 1). These methods are complementary, XRF providing elemental composition, and FORS providing molecular or structural information. The XRF spectra are examined using traditional methods, i.e. peaks in the XRF spectra are assigned

Table 1 Summary of analytical results regarding pigment identification. Angle tolerance values refer to the spectral maps in Figs. 1–4. In the XRF column, pigments listed in boldface are those most likely responsible for the visible appearance (color) of the analyzed areas. Key: Major, Minor, (trace). In the 'possible assignment' column: (from underlying layer).

		Imaging spectroscopy and FORS		XRF	
	Region	Tol.	Possible assignment	Elements	Possible assignment
1	Dark blue floor	0.1	Azurite	**Cu**, Fe, Zn, (Si, K, Ca, Ti, Mn, Pb)	**Azurite**, iron earth
2	Blue floor, border, and corners	0.18	Azurite	**Cu**, Fe, Zn, (Si, K, Ca, Ti, Mn, Pb)	**Azurite**, iron earth
3	Blue around Christ	0.1	Azurite and ultramarine	**Cu**, **Pb**, Al, Si, K, Ca, Fe, Zn, (Ti, Mn)	**Azurite**, **lead white**, **ultramarine**, iron earth
4	Blue highlights	0.15	Ultramarine		
5	Dark green	0.144	Copper containing green (verdigris or Cu-resinate)	**Cu**, **Pb**, Ca, (Sn, Cl, Fe)	**Cu-containing green**, azurite, (lead-tin yellow), lead white
6	Green	0.08	Copper containing green (verdigris or Cu-resinate)	**Cu**, **Pb**, Sn, (Si, Ca, Cl, Fe)	**Cu-containing green**, **lead-tin yellow**, azurite, lead white
7	Brown	0.06	Iron oxide		
8	White robes	0.08	Lead white		
9	Faces and hands	0.08	Terre verte?		
10	Yellow	0.056	Lead-tin yellow or organic dye, lead white	**Pb**, Sn, (Si, Fe)	**Lead-tin yellow**, lead white
11a	Red robes	0.08	Red lead	**Pb**, (Ca, Fe, Cu)	**Red lead**
11b	Dark red	0.08	Red lead on black		
12	Black halo lines	0.22	Iron-based ink		
13	Purple	0.1	Azurite and organic dye	**Ca**, **Cu**, **Pb**, Au, (Mn, Fe, Zn)	**Organic red dye + chalk**, **azurite**, lead white, (gold leaf)
14	Red book	0.137	Organic dye		
15	Red book and border	0.1	Organic dye	**Ca**, S, Cu, Pb, (K, Fe)	**Organic red dye + chalk**, gypsum
16	Pink	0.06	Organic dye and lead white	**Pb**, **Ca**, (Fe, Cu)	**Organic red dye + chalk**, **lead white**
17	Dark pink	0.04	Organic dye and lead white		

to the presence of specific chemical elements, and possible pigments inferred by comparison with databases while taking into account possible effects of paint layering and shielding by heavy elements. The FORS spectra are compared with various in-house and public databases (Clark *et al.*, 2007; CNR-IFAC, 2011), which contain minerals as well as pure and mixed pigments painted out on various supports including parchment. Typically FORS spectra are acquired from several sites within each defined regions.

Assignment of blue endmembers

The analysis found four blue endmembers: endmembers 1 and 2 are assigned to light and dark azurite, endmember 3 to ultramarine layered over azurite, and endmember 4 to pure ultramarine (see below) (Fig. 2).

Endmembers 1 and 2 (blue maps and blue in Figs. 2A, B) differ in the level of brightness but have the same spectral shape; they map to the background, the majority of the robe of the apostle on Christ's proper left (likely St John; Nordenfalk, 1975), the outer portion of the *mandorla* surrounding Christ, and the blue border elements. The FORS spectra (Fig. 2C) from sites within these endmember maps all have a peak reflectance at 467 nm and low reflectance from 600 to 900 nm with a subsequent rise at longer wavelengths. From about 1100 to 2400 nm, all the FORS spectra acquired on the miniature are dominated by broad absorption features attributable to the parchment support (Ricciardi *et al.*, 2009). The FORS spectra corresponding to the first two blue endmembers also feature three narrow absorption features at 1498, 2284, and 2351 nm. The overall spectral shape and the position of the three vibrational bands are a good match for the mineral azurite (a basic copper carbonate), with the bands deriving from –OH and $–CO_3$ vibrational overtones and combination (Hunt & Salisbury, 1971). The XRF spectra (e.g. sp11 in Fig. 2D) contain a dominant amount of copper (Cu), consistent with azurite, the most likely Cu-containing blue pigment available in the fourteenth century. The XRF spectra also contain elements consistent with the presence of mineral earths, as well as a small amount of zinc (Zn). SEM–EDS analysis of a small sample taken from the upper right corner of the blue border reveals that the Zn is present on some areas of the azurite particles and not as zinc white, an anachronistic modern pigment. The Zn may be present in small crystals of smithsonite ($ZnCO_3$) known to naturally occur with azurite ores (Anthony *et al.*, 2003). The presence of Zn in the azurite concurs with analyses performed by conservation scientists at the Getty Museum on another illuminated manuscript leaf by Pacino di Buonaguida belonging to the same *laudario* (Trentelman, 2009).

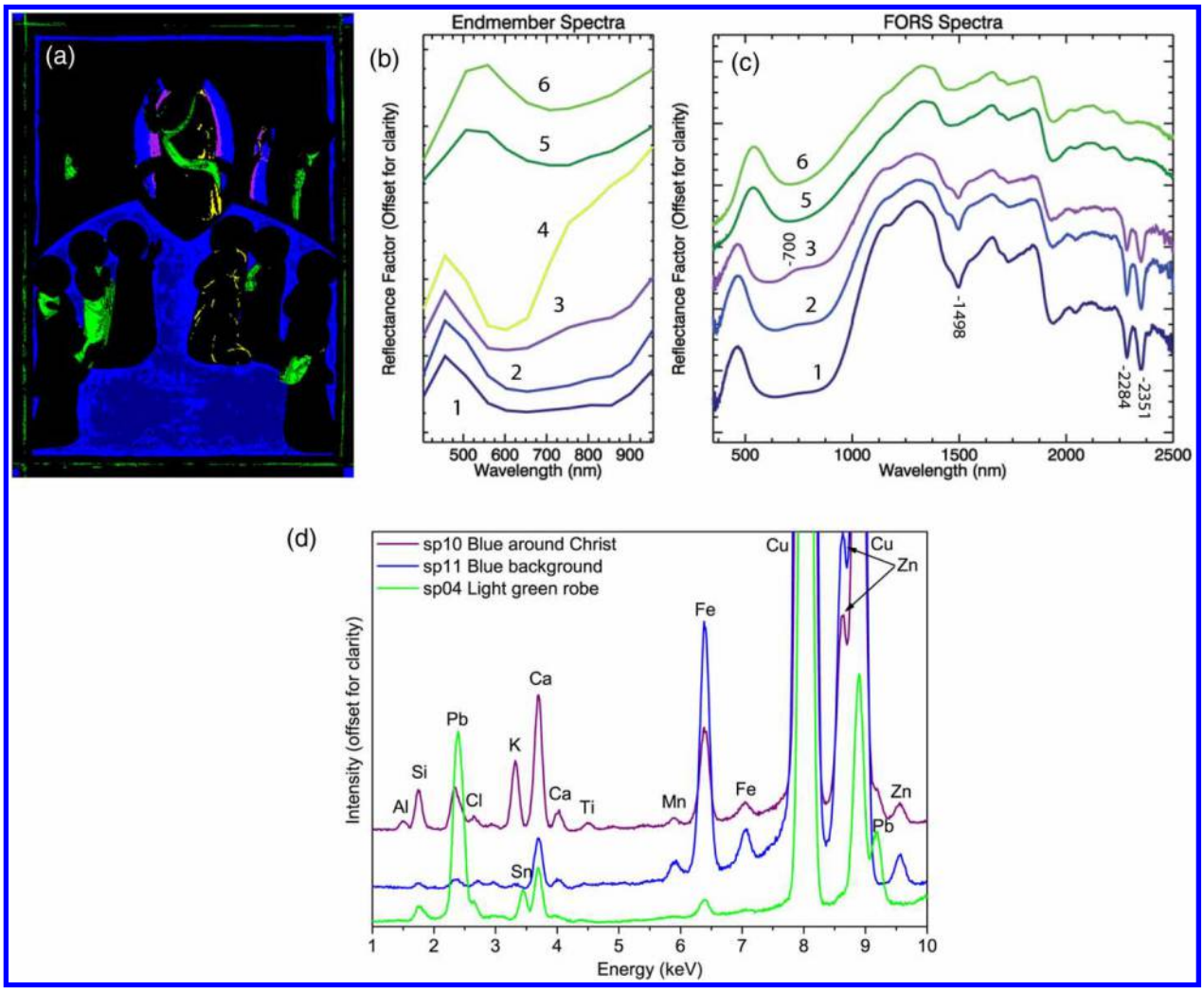

Figure 2 Maps and spectra of the blue and green endmembers. (A) Endmember map representing the (B) blue and green endmember spectra; (C) associated FORS spectra from sites defined by the maps; (D) XRF spectra from sites in the green, blue, and purple map regions. The results indicate that blue fields (1, 2) are painted with azurite except in the area around Christ (3), which has ultramarine layered on top of the azurite. Ultramarine is also used for the blue highlights on Christ (4). The green areas (5, 6) all have the same reflectance spectral shape, corresponding to a Cu-based green likely mixed with a yellow pigment, which can probably be identified as lead-tin yellow based on the XRF spectra.

Endmember 3 maps to the inner portion of the *mandorla* around Christ and to very dark highlights on the left side and belt of St John's robe (purple map and spectrum in Fig. 2). The FORS spectrum here also matches azurite, but there is a moderate increase in reflectance between 700 and 950 nm, which can be indicative of a layering of ultramarine over azurite. Paintouts of varying thickness of ultramarine on top of azurite were found to match the FORS spectral shape (Picollo *et al.*, 2010). The XRF spectrum (sp10 in Fig. 2D) is consistent with the presence of azurite (Cu) and ultramarine (Al, Si, and K) with some lead white (Pb). These results can be interpreted as a thin layer of ultramarine applied on top of azurite in selected areas to achieve the deeper blue color. This sequencing of paint layers is not unexpected since ultramarine glazing over azurite was a common technique during this time period (Roy, 1993).

Endmember 4 (yellow) has the highest reflectance in the NIR and maps to dark blue outlines and drapery folds on the white mantles of Christ and of the apostle Bartholomew (Nordenfalk, 1975) (yellow map and spectrum in Fig. 2). This reflectance spectrum is characteristic of ultramarine, which has a transition to high reflectance at ~700 nm. Although these areas were too small to measure using FORS, it is not unlikely that pure ultramarine was used for highlights. Microscopic observation reveals deep blue ultramarine particles of varying size with trace sightings of colorless crystalline impurities suggesting the pigment is of a high quality (Roy, 1993).

Assignment of green endmembers

Green garments visible in Christ and six of the apostles consist of a light green pigment with dark green brushstrokes applied over it to render drapery shadows (Fig. 2). This visible color shift between light and

dark green produces two green endmembers (5, 6) that are spectrally similar except for a difference in slope from 400 to 450 nm. The first maps (5) to the dark green areas, mostly correlating to the drapery shadows in the robes of the figures, and the second (6) to the light green color used to render the robes as well as a perimeter (green map and spectra in Fig. 2). The FORS spectra from sites defined by these two maps have a peak reflectance at 536–540 nm and a slow rise at 800–1300 nm, and thus best match a Cu-containing green such as verdigris or copper resinate. The presence of malachite, another Cu-containing green, is unlikely since the characteristic absorption features around 2215 and 2270 nm (Hunt & Salisbury, 1971) are not observed. XRF spectra from sites in the two maps also point to a Cu-containing green with lead-tin yellow and perhaps some lead white. Alternatively, the XRF spectra could be interpreted as being a mixture of azurite with lead-tin yellow (since multiple pigments can have the same elemental composition), but the FORS spectra rule out the presence of azurite since its characteristic vibrational bands are not observed. In addition, the Zn peak, present in the azurite, was not observed in the green. The Sn peak in the XRF spectra is largest for the light green, suggesting that an increased amount of lead-tin yellow gives rise to the brighter, light green hues. The use of lead-tin yellow also favors an assignment to verdigris or copper resinate (rather than malachite), since both are transparent and were often used in mixtures with lead-tin yellow (Roy, 1993).

Assignment of brown, white, flesh tone, yellow, red, and black endmembers

The brown endmember (7) has the characteristic spectral shape of an iron oxide pigment, including two reflectance peaks at ~600 and ~750 nm, and maps to a mantle and robe of two of the apostles (brown map and spectrum in Fig. 3). FORS spectra from sites in this map have a transition edge at 555 nm, a minor peak at 597 nm, and a major reflection peak at 761 nm and absorption bands at 649 and 916 nm assignable to forbidden Laporte transitions, all consistent with the assignment to an iron oxide pigment (Clark, 1999).

The white endmember (8), which maps to the white mantles of Christ and the apostle Bartholomew, is broad with some increased absorption at 400 nm (white map and black spectrum in Fig. 3). The FORS spectra of sites within this map all have a vibrational feature at 1447 nm (Bacci *et al*., 2007a, b) and non-zero reflectance at 350 nm, indicative of lead white. However, the FORS from the site on Christ's mantle has a visible peak reflectance at 500 nm, and small absorption features at 1495, 2285,

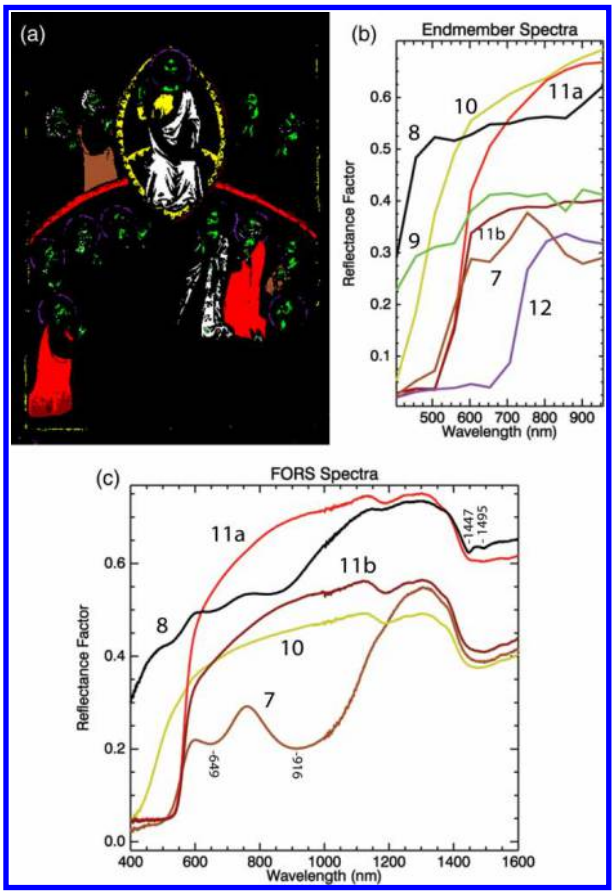

Figure 3 Maps and spectra of the brown, white, flesh tone, yellow, red, and black endmembers. (A) Endmember map representing the (B) endmember spectra; (C) associated FORS spectra from sites defined by the maps. The maps and site analysis find the brown cloak (7) is painted with an iron oxide pigment, the white robes (8) are lead white, yellow areas (10) are similar spectrally and are lead-tin yellow, the red robes (11a, 11b) are red lead but shading with a dark pigment underneath is also found in the robe of the lower left apostle. A black outline on the halos (12) shows a spectrum indicative of an iron-based ink.

and 2348 nm indicative of the presence of some azurite (Hunt & Salisbury, 1971). The FORS from the apostle Bartholomew's mantle has these same vibrational features associated with a small amount of azurite as well as stronger reflectance features matching those of the iron oxide brown discussed above. Brown earths were often employed for shadows and outlines.

The faces and hands of Christ and the apostles all have a common flesh tone endmember (9) spectrum similar to the white endmember but with a small transition around 575 nm (green spectrum and map in Fig. 3). These sites are too small to be analyzed with FORS, and are expected to consist of a complex-layered structure. The endmember has spectral features compatible with *terre verte* and visual inspection under the microscope reveals a complex layering of paint. This consists of a homogeneous layer of green (most likely *terre verte*) acting as foundation, a light

pink layering of individual brushstrokes used to render facial features, and white highlights painted selectively to suggest Christ's light touching the face of each apostle. A brown earth is employed to delicately outline each figure's hairline, eyes, nose, mouth, facial profile, and to crosshatch neckline shadows.

The yellow endmember (10) show a biphasic rise in the visible to NIR and maps to the *mandorla* around Christ and to his robe (yellow map and spectrum in Fig. 3). Historically, the most likely candidate yellow pigments include lead-tin yellow, massicot (PbO), orpiment (As_2S_3), or an organic dye. The FORS spectra show two inflection points at ~475 and ~560 nm, suggesting the presence of either lead-tin yellow or a dye, while orpiment and massicot can be ruled out as they have transmission edges at 525–545 nm and ~450 nm, respectively. The presence of Pb and Sn in the XRF spectra leads to the assignment of the pigment as lead-tin yellow.

The red endmembers (11a, 11b) have a sharp transition at ~550 nm and map to the mantles of two apostles (light and dark red spectra and maps in Fig. 3). The only difference between the two is the amount of reflectance above 600 nm. The endmember with lower reflectance maps to a darker area at the bottom of one of the mantles. The FORS spectra from these sites show an inflection point at 565–567 nm, which best matches red lead (Pb_3O_4) rather than vermilion (HgS, inflection point at 580–605 nm). XRF shows that the dominant element in the spectra is lead, and no mercury (Hg) is detected; this is also consistent with the presence of red lead.

An unexpected endmember (12), which maps to the dark outline of the gold halos, was found during image processing (purple spectrum and map in Fig. 3). The dark line reinforces the simple circular arrangement of punch work used to depict the halos of Christ and eight of the apostles. The endmember spectrum has near zero reflectance from 400 to 700 nm and then a transition to higher reflectance at ~750 nm. These areas are too narrow to measure with FORS, however the endmember spectrum is compatible with an iron-based ink (e.g. iron-gall).

Assignment of the purple and luminescent pink and red endmembers

The luminescence image (Fig. 4A) is obtained by excitation with blue-green light and collected at 700 nm to minimize emission from the paint binders and parchment support. Bright luminescence is observed in the red border, the book held by Christ, and the pink robes of the apostles. Note that bright luminescence from the exposed parchment is also seen in a few areas of loss in the gold leaf, as expected. Highlights on robes, especially the pink and purple ones, are also luminescent, as are the inner side of the orange arc and the scalloped detail in the *mandorla* around Christ. Most of these luminescent areas are mapped by five reflectance endmembers.

Purple endmember 13 (teal map and spectrum in Fig. 4) maps to three mantles and one robe of the apostles. The corresponding FORS spectra show a peak at 496 nm, an absorption feature at 560 nm followed by a plateau, and then an inflection point at ~700 nm. Vibrational features in the NIR at ~1488, 2284, and 2348 nm indicate the presence of azurite (see discussion of blue endmembers), but the inflection at 700 nm does suggest the possibility that some ultramarine could have been used in the mixture. The first derivative shows maxima at 585, 695, and 936 nm. The absorption feature at 560 nm and inflection at 585 nm are consistent with a red dye as was noted for the red and pink luminescent endmembers (see below). Examination of the luminescence image suggests some weak emission from the purple robes. If the 560 nm feature is taken as an $n \rightarrow \pi^*$ transition, then this dye could be identified as carmine, an insect-derived anthraquinone (Bisulca *et al.*, 2008). An XRF spectrum from a site in the purple map shows Pb, Cu, and Ca as the major elements, consistent with the presence of lead white, azurite, and a red dye precipitated with chalk.

The pink endmembers 16 and 17 map to the mantles and robes of seven of the apostles (pink and purple spectra and maps in Fig. 4). The FORS spectra from these regions all show a rise in reflectance from 350 to ~550 nm and an absorption feature at 560 nm along with a rise in reflectance in the red. There is also a small peak at 1448 nm suggesting the presence of lead white. The first derivatives of these spectra have a broad asymmetric band with a maximum at 590 nm (FWHM ~50 nm), in contrast to vermillion or red lead. The spectral shape and especially the presence of luminescence are suggestive of the presence of an organic red dye. If the 560 nm absorption feature is assigned to an $n \rightarrow \pi^*$ transition, the dye used could be carmine (Bisulca *et al.*, 2008). XRF spectra from sites defined by the pink endmembers show mostly Pb and Ca, which is consistent with the presence of lead white and a red dye with chalk ($CaCO_3$) as the possible substrate.

Endmembers 14 and 15 associated with the red book held by Christ and the red border can similarly be assigned to a dye (light and dark brown spectra and maps in Fig. 4). The FORS spectra from these sites have similar spectral shapes, including the first derivative, as the pink endmembers, but have less absorption at 1448 nm indicating less lead white is present. This is also reflected in the more transparent appearance of these areas as compared with the pink robes.

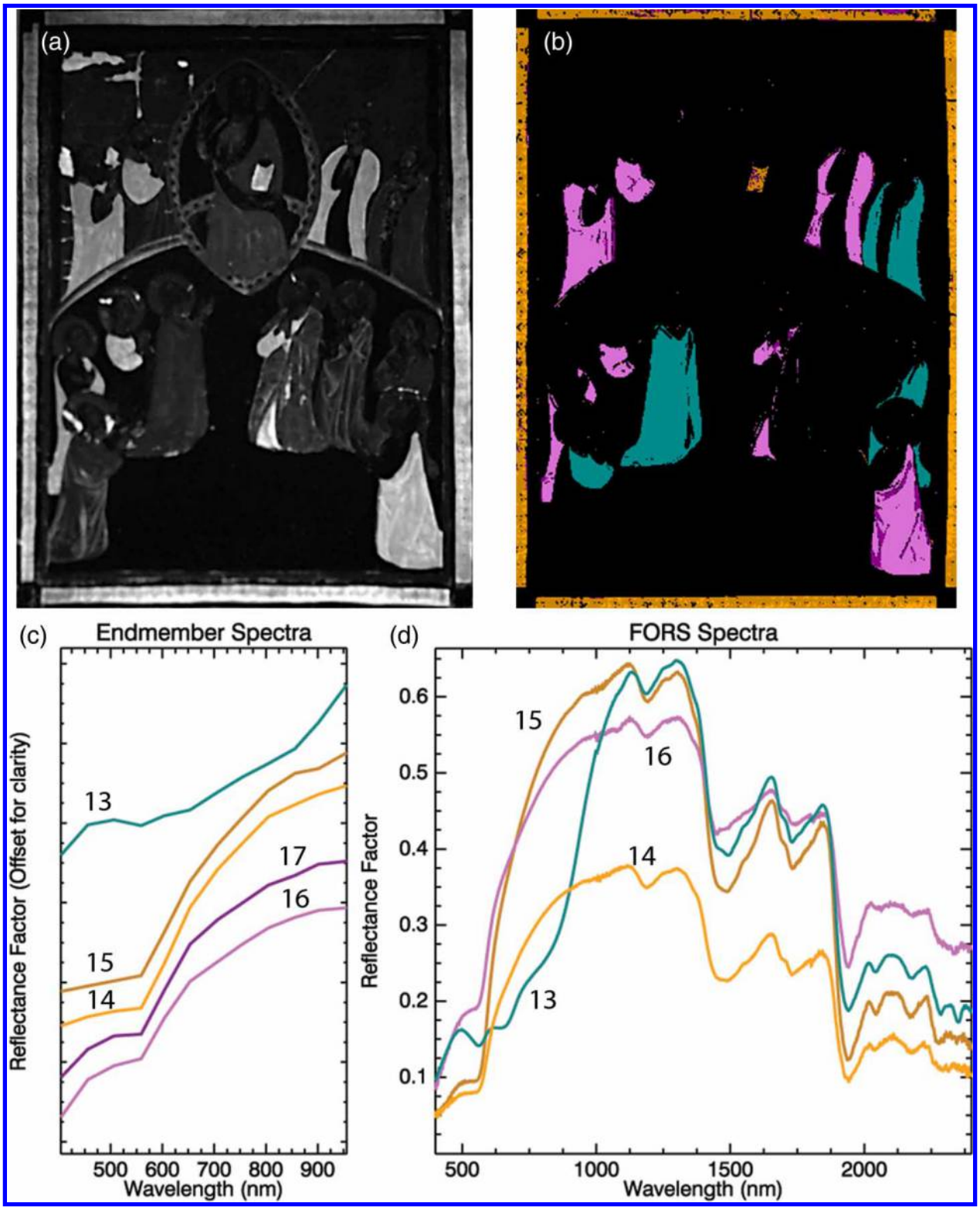

Figure 4 The luminescence image, maps, and spectra of the purple and luminescent pink and red endmembers. (A) Luminescence image at 700 nm; (B) endmember map representing the (C) endmember spectra; (D) associated FORS spectra from sites defined by the maps. The purple cloaks (13) are spectrally similar and are obtained with azurite mixed with a red organic dye. The red book and border (14, 15) are both painted with a red organic dye with varying amounts of dye and similarly the pink robes are also painted with a red dye mixed with varying amounts of lead white.

Conclusion

The results from this study suggest that automatic clustering of low spectral and spatial resolution image cubes can be used to provide a more objective and unbiased analysis method to identify areas having common reflectance spectral properties in both the visible and NIR. While a recent imaging spectroscopy study of a twentieth-century painting (Delaney *et al.*, 2010) required smaller spectral sampling intervals and extension into the infrared, the relatively limited

number of possible pigments and simple mixtures which are found on illuminated manuscripts, with the addition of site-specific FORS analysis, loosens this requirement. This study shows once again that the fusion of FORS and XRF data can yield more robust assignments of paint compositions in illuminated manuscripts than use of either technique alone (Ricciardi *et al*., 2009). The results here also contribute to the understanding of the palette used by Pacino di Buonaguida's workshop, with the finding of azurite, lead-tin yellow, red lead, an organic red dye (likely carmine, an insect-derived anthraquinone), a copper-containing green, brown iron oxide, and lead white. These results are mostly consistent with those reported by researchers studying Pacino's illuminations and panel paintings at the Getty Museum, although they have not reported evidence for use of red dyes or a copper-based green in the manuscript leaves studied to date (Szafran *et al*., 2011).

In this study the spatial sampling was limited to 0.3 mm per pixel owing to the need to manually register the spectral image frames, which results from chromatic errors in the lens and from offsets induced by the filters. Clearly, a more robust approach would benefit from finer spatial sampling and an image-based registration process to improve spatial and spectral quality. Ongoing studies are addressing these issues through the use of an optimized registration algorithm (Conover *et al*., 2011).

Acknowledgments

The authors acknowledge funding by the Andrew W. Mellon and Samuel H. Kress foundations. Reference paintout samples were made by Brian Baade. We acknowledge advice and reference materials from Marcello Picollo and Maurizio Aceto. Finally, we dedicate this paper to Mr Ross Merrill, former Chief of Conservation, National Gallery of Art, Washington, DC whose vision has helped guide our studies in the application of imaging spectroscopy to conservation.

References

Aceto, M., Agostino, A., Bianco, V., Pellizzi, E., Gulmini, M. & Castronovo, S. 2008. An Interdisciplinary, Non-Invasive Study on Ten Manuscripts Coming from the San Colombano Abbey in Bobbio. In: A. Gueli, ed. *Proceedings AIAr Conference, V Congresso Nazionale di Archeometri, Scienza e Bieni Culturali, Siracusa, Sicilia*, *26–29 February, 2008*. Rome: Morrone Editoire, pp. 91–103.

Anthony, J.W., Bideaux, R.A., Bladh, K.W. & Nichols, M.C. eds. 2003. *Handbook of Mineralogy*. Chantilly, VA: Mineralogical Society of America. [accessed 22 December 2012]. Available at: <http://www.handbookofmineralogy.org/>

Appolonia, L., Vaudan, D., Chatel, V., Aceto, M. & Mirti, P. 2009. Combined Use of FORS, XRF and Raman Spectroscopy in the Study of Mural Paintings in the Aosta Valley (Italy). *Analalytical and Bioanalytical Chemistry*, 395:2005–13.

Ashley-Smith, J., Derbyshire, A. & Pretzel, B. 2002. The Continuing Development of a Practical Lighting Policy for Works of Art on Paper and Other Object Types at the Victoria and Albert Museum. In: R. Vontobel, ed. *ICOM Committee for Conservation, 13th Triennial Meeting, Preprints*. London: James & James, vol. l, pp. 3–8.

Attas, M., Cloutis, E., Collins, C., Goltz, D., Majzels, C., Mansfield, J.R., *et al.* 2003. Near-Infrared Spectroscopic Imaging in Art Conservation: Investigation of Drawing Constituents. *Journal of Cultural Heritage*, 4: 127–36.

Bacci, M., Picollo, M., Radicati, B., Aldrovandi, A. & Migliori, A. 2007a. Studio dei materiali pittorici del Graduale 558 mediante tecniche spettroscopiche non invasive. In: M. Scudieri & S. Giacomelli, eds. *Fra Giovanni Angelico: pittore miniatore o miniatore pittore?* Firenze: Giunti Editore S.p.A, pp. 100–11.

Bacci, M., Picollo, M., Trumpy, G., Tsukada, M. & Kunzelman, D. 2007b. Non-invasive Identification of White Pigments on 20th Century Oil Paintings by Using Fiber Optic Reflectance Spectroscopy. *Journal of the American Institute for Conservation*, 46: 27–37.

Baronti, S., Casini, A., Lotti, F. & Porcinai, S. 1998. Multispectral Imaging System for the Mapping of Pigments in Works of Art by use of Principal-Component Analysis. *Applied Optics*, 37: 1299–309.

Bisulca, C., Picollo, M., Bacci, M. & Kunzelman, D. 2008. UV-VIS-NIR Reflectance Spectroscopy of Red Lakes in Paintings. In: *9th International Conference of NDT of Art, Jerusalem, Israel, 25–30 May 2008* [accessed 22 December 2012]. Available at: <www.ndt.net/article/art2008/papers/199Bisulca.pdf>

Boardman, J.W., Kruse, F.A. & Green, R.O. 1995. Mapping Target Signatures via Partial Unmixing of AVIRIS Data. In: V.J. Realmuto, ed. *Summaries of the Fifth Annual JPL Airborne Earth Science Workshop*. Washington: JPL, vol. 1, pp 23–6.

Berns, R.S. 2005. Color-Accurate Image Archives Using Spectral Imaging. In: National Academy of Sciences, ed. *Scientific Examination of Art – Modern Techniques in Conservation and Analysis*. Washington, DC: The National Academies Press, pp. 120–36.

Casini, A., Lotti, F., Picollo, M., Stefani, L. & Buzzegoli, E. 1999. Image Spectroscopy Mapping Technique for Non-Invasive Analysis of Paintings. *Studies in Conservation*, 44: 39–48.

Casini, A., Bacci, M., Cucci, C., Lotti, F., Porcinai, S., Picollo, M., Radicati, B., Poggesi, M. & Stefani, L. 2005. Fiber Optic Reflectance Spectroscopy and Hyper-spectral Image Spectroscopy: Two Integrated Techniques for the Study of the Madonna dei Fusi. In: R. Salimbeni & L. Pezzati, eds. *Proceedings of SPIE, O3A: Optical Methods for Arts and Archaeology*. Bellingham, WA: SPIE, vol. 5857; pp. 58570M1–07M8.

Clark, R.N. 1999. Spectroscopy of Rocks and Minerals, and Principles of Spectroscopy. In: A.N. Rencz, ed. *Manual of Remote Sensing, Remote Sensing for the Earth Sciences*. New York: John Wiley and Sons, vol. 3, pp. 3–58.

Clark, R.N., Swayze, G.A., Wise, R., Livo, E., Hoefen, T., Kokaly, R. & Sutley, S.J. 2007. *USGS Digital Spectral Library splib06a*. Denver: U.S. Geological Survey, Digital Data Series 231 [accessed 22 December 2012]. Available at: <http://speclab.cr.usgs.gov/spectral.lib06/ds231/index.html>

CNR-IFAC. 2011. Fiber Optics Reflectance Spectra Database of Pictorial Materials in the 270 to 1700 nm Range [accessed 22 December 2012]. Available at: <http://fors.ifac.cnr.it/>

Conover, D., Delaney, J.K., Ricciardi, P. & Loew, M.H. 2011. Towards Automatic Registration of Technical Images of Works of Art. In: D. Stork, J. Coddington & A. Bentkowska-Kafel, eds. *Proceedings of SPIE, Computer Vision and Image Analysis of Art II*. Bellingham, WA: SPIE, vol. 7869, pp. 78690–9.

Delaney, J.K., Walmsley, E., Berrie, B.H., Fletcher, C.H. 2005. Multispectral Imaging of Paintings in the Infrared to Detect and Map Blue Pigments. In: National Academy of Sciences , ed. *Scientific Examination of Art – Modern Techniques in Conservation and Analysis*. Washington, DC: The National Academies Press. pp. 120–36.

Delaney, J.K., Facini, M., Glinsman, L.D. & Thoury, M., 2009a. Application of Imaging Spectroscopy to the Study of Illuminated Manuscripts. Poster at American Institute For Conservation 37th Annual Meeting. Los Angeles, 20 May 20.

Delaney, J.K., Zeibel, J.G., Thoury, M., Littleton, R., Morales, K.M., Palmer, M. & de la Rie, E.R. 2009b. Visible and Infrared Reflectance Imaging Spectroscopy of Paintings: Pigment Mapping and Improved Infrared Reflectography. In: L. Pezzati & R. Salimbeni, eds. *Proceedings of SPIE, O3A: Optics for Arts, Architecture, and Archaeology II*. Bellingham, WA: SPIE, vol. 7391, pp. 739103–8.

Delaney, J.K., Zeibel, J.Z., Thoury, M., Littleton, R., Palmer, M., Morales, K.M., de la Rie, E.R. & Hoenigswald, A. 2010. Visible and Infrared Imaging Spectroscopy of Picasso's Harlequin Musician: Mapping and Identification of Artist Materials in situ. *Applied Spectroscopy*, 64: 584–94.

Dirk, C.W., Delgado, M.F., Olguin, M. & Druzik, J. 2009. A Prism-Grating-Prism Spectral Imaging Approach. *Studies in Conservation*, 54: 77–89.

Fischer, C. & Kakoulli, I. 2006. Multispectral and Hyperspectral Imaging Technologies in Conservation: Current Research and Potential Applications. *Reviews in Conservation*, 7: 3–16.

France, F.G. 2011. Advanced Spectral Imaging for Noninvasive Microanalysis of Cultural Heritage Materials: Review of Application to Documents in the U.S. Library of Congress. *Applied Spectroscopy*, 65: 565–74.

Havermans, J., Aziz, H.A. & Scholten, H. 2003. Non Destructive Detection of Iron-gall Inks by Means of Multispectral Imaging. Part 2: Application on Original Objects Affected with Iron-gall-ink Corrosion. *Restaurator*, 23: 88–94.

Hunt, G.R. & Salisbury, J.W. 1971. Visible and Near Infrared Spectra of Minerals and Rocks. II. Carbonates. *Modern Geology*, 2: 23–30.

Kanter, L.B., Drake Boehm, B., Brandon Strehlke, C., Freuler, G., Mayer Thurman, C.C. & Palladino, P. 1994. *Painting and Illumination in Early Renaissance Florence 1300–1450*. New York: Metropolitan Museum of Art. pp. 58–63.

Klein, M.E., Aalderink, B.J., Padoan, R., De Bruin, G. & Steemers, T.A. 2008. Quantitative Hyperspectral Reflectance Imaging. *Sensors*, 8: 5576–618.

Melessanaki, K., Papadakis, V., Balas, C. & Anglos, D. 2001. Laser Induced Breakdown Spectroscopy and Hyper-spectral Imaging Analysis of Pigments on an Illuminated Manuscript. *Spectrochimica Acta B*, 56: 2337–46.

Mrusek, R., Fuchs, R. & Oltrogge, D. 1995. Spektrale Fenster zur Vergangenheit – Ein neues Reflektographieverfahren zur Untersuchung von Buchmalerei und historischem Schriftgut. *Naturwissenschaften*, 82: 68–79.

Nordenfalk, C. 1975. *Medieval and Renaissance Miniatures from the National Gallery of Art*. Washington, DC: National Gallery of Art, pp. 22–5.

Padoan, R., Klein, M.E., de Bruin, G., Aalderink, B.J. & Steemers, T.A.G. 2010. Quantitative Hyperspectral Study of the Anjou Bible. In: L. Watteeuw & J. Van der Stock, eds. *The Anjou Bible: A Royal Manuscript Revealed*. Leuven, Belgium: Peeters, pp. 171–85.

Panayotova, S. 2009. New Miniatures by Pacino di Buonaguida in Cambridge. *Burlington Magazine*, CLI: 144–48.

Picollo, M., Ricciardi, P. & Delaney, J.K., 2010. *Florence: CNR-IFAC [unpublished report]*. Washington, DC: National Gallery of Art.

Ricciardi, P., Delaney, J.K., Glinsman, L.D., Thoury, M., Facini, M. & de la Rie, E.R. 2009. Use of Visible and Infrared Reflectance and Luminescence Imaging Spectroscopy to Study Illuminated Manuscripts: Pigment Identification and Visualization of Underdrawings. In: L. Pezzati & R. Salimbeni, eds. *Proceedings of SPIE, O3A: Optics for Arts, Architecture, and Archaeology II*. Bellingham, WA: SPIE, vol. 7391, pp. 739106–12.

Roy, A. ed. 1993. *Artists' Pigments. A Handbook of their History and Characteristics*. Washington, DC: National Gallery of Art, vol. 2, pp. 39–44, 132.

Szafran, Y., Namowicz, C., Schmidt Patterson, C., Sciacca, C., Trentelman, K. & Turner, N. 2011. Painting on Parchment and Panel: An Exploration of Pacino di Bonaguida's Technique. In: M. Spring, ed. *Studying Old Master Paintings: Technology and Practice*. London: Archetype. pp. 8–14.

Trentelman, K. 2009. Personal communication. Los Angeles: Getty Conservation Institute.

Zhao, Y., Berns, R.S., Taplin, L.A. & Coddington, J. 2008. An Investigation of Multispectral Imaging for the Mapping of Pigments in Paintings. In: D. Stork & J. Coddington. eds. *Proceedings of SPIE, Computer Image Analysis in the Study of Art*. Bellingham, WA: SPIE, vol. 6810, pp. 681007.